# Shear Tests of Rivet Fastened Rectangular Hollow Flange Channel Beams

Poologanathan Keerthan and Mahen Mahendran
*Queensland University of Technology (QUT), Brisbane, Australia*

**Abstract:** The intermittently rivet fastened Rectangular Hollow Flange Channel Beam (RHFCB) is a new cold-formed hollow section proposed as an alternative to welded hollow flange channel beams. It is a monosymmetric channel section made by intermittently rivet fastening two torsionally rigid rectangular hollow flanges to a web plate. This process enables the end users to choose an effective combination of different web and flange plate sizes to achieve optimum design capacities. Recent research studies focused mainly on the shear behaviour of the most commonly used lipped channel beam and welded hollow flange beam sections. However, the shear behaviour of rivet fastened RHFCB has not been investigated. Therefore a detailed experimental study involving 24 shear tests was undertaken to investigate the shear behaviour and capacities of rivet fastened RHFCBs. Simply supported test specimens of RHFCB with aspect ratios of 1.0 and 1.5 were loaded at mid-span until failure. Comparison of experimental shear capacities with corresponding predictions from the current Australian cold-formed steel design rules showed that the current design rules are very conservative for the shear design of rivet fastened RHFCBs. Significant improvements to web shear buckling occurred due to the presence of rectangular hollow flanges while considerable post-buckling strength was also observed. Such enhancements to the shear behaviour and capacity were achieved with a rivet spacing of 100 mm. Improved design rules were proposed for rivet fastened RHFCBs based on the current shear design equations in AISI S100 and the direct strength method. This paper presents the details of this experimental investigation and the results.

Keywords: *Cold-formed steel beams, Rivet fastened hollow flange channel beams, Shear capacity, Experiments, Design equations, Direct strength method.*

*Corresponding author's email address:* m.mahendran@qut.edu.au

# 1. Introduction

The use of cold-formed steel members in low rise building construction has increased significantly in recent times. It has been suggested that in the future more than 70% of the steel buildings will be constructed using cold-formed steel. The cold-formed steel manufacturers have continuously utilised thin high strength steels and new manufacturing technologies to develop advanced light weight sections that are more structurally efficient and cost-effective in order to improve the market share for cold-formed steel construction. Cold-forming process is simple, efficient, economical and environmentally friendly, which is capable of manufacturing very effective sections compared to the hot-rolled open steel sections. The Rectangular Hollow Flange Channel Beam (RHFCB) is one such advanced light weight section introduced recently by cold-formed steel manufacturers and researchers.

In 2005 OneSteel Australian Tube Mills (OATM, 2008) introduced the first RHFCB section, known as the LiteSteel beam (LSB) primarily for use as flexural members in residential and light commercial/industrial applications (see Figure 1). LSB is manufactured from a single strip of high strength steel using a combined cold-forming and dual electric resistance welding process. The LSBs combine the stability of hot-rolled sections with the high strength to weight ratio of cold-formed sections, and are very efficient as structural beams since they have the hollow flanges away from the centre. In the past, the LSB has been highly researched due to its ability to provide capacities that are more typically associated with hot-rolled, than cold-formed steel members (Keerthan and Mahendran, 2008, 2010a, 2010b and 2011; Keerthan et al. 2014a, 2014b and 2014c; Anapayan et. al. 2011; Anapayan and Mahendran, 2012a and 2012b; Seo and Mahendran, 2011 and 2012). However, the OATM discontinued LSB production in 2012, mostly due to the expensive manufacturing cost associated with the dual electric resistance welding process.

The LSB sections are efficient and attractive steel products, which can be used in floor and roof systems as well as in modular building systems. Although the LSBs are no longer produced, there is a need to find an alternative manufacturing method to produce equivalent sections due to their popularity and demand among architects, engineers and builders in recent times. In this research study, an alternative manufacturing method has been proposed based on a combined cold-forming and rivet fastening process to produce RHFCBs (Figure 2) thus eliminating the costly dual electric resistance welding process.

The rivet fastened RHFCB shown in Figure 2 is a mono-symmetric section where the rectangular hollow flanges are cold-formed first and then connected to the web plate using rivet fastening. Due to this simple and flexible manufacturing process, the designers can effectively choose different plate dimensions and thicknesses for web and flange elements to achieve the most efficient section to suit the clients' requirements. As an example, selecting a thicker web plate element is likely to eliminate or delay the unique lateral distortional buckling observed in hollow flange beams (Anapayan and Mahendran, 2012a). Unlike for LSBs with only three hollow flanges (45x15 mm, 60x20 mm and 75x25 mm) the rivet fastened RHFCBs can be produced with many different hollow flange sizes. In addition to these features, they have additional flange lips that are used for rivet fastening, which may enhance their design capacities. However, limited investigation has been carried out on the structural behaviour and strength of rivet fastened RHFCBs.

For the newly developed rivet fastened RHFCB sections to be used as flexural members, their flexural and shear capacities need to be fully investigated. In this research the shear behaviour and capacity of rivet fastened RHFCB was investigated using experimental studies. The web shear buckling design is based on the assumption that the web elements are simply supported, in which the effect of flange rigidity is neglected in conventional lipped channel beams (LCB). LaBoube and Yu (1978) calculated the ultimate strengths of LCBs by assuming that the web-flange joints are simply supported. However, Keerthan and Mahendran (2010a, 2010b and 2013) found that there is considerable fixity at the web to flange juncture, in particular for welded hollow flange channel beams. They also showed the presence of significant post-buckling shear strength for welded hollow flange channel beams. However, intermittent rivet fastening instead of continuous welding of flanges to web elements may reduce these beneficial effects on the shear capacity. Hence this research investigated the shear capacities of rivet fastened RHFCBs. This paper presents the details of a series of primarily shear tests of rivet fastened RHFCBs, and the results. Experimental shear capacities are compared with the predicted shear capacities using the current design rules. Suitable design rules are then developed based on the current shear design equations in AISI S100 (AISI, 2012) and the direct strength method (DSM).

## 2. Shear Capacities of Lipped Channel Beams and Hollow Flange Beams

In the past the shear buckling capacities of conventional lipped channel beams (LCBs) are computed by neglecting the effect of flange rigidity. LaBoube and Yu (1978) investigated the shear strength of cold-formed steel LCBs by considering different web slenderness ratio, the edge support conditions provided by the flanges with varying flat width-to-thickness ratios and the mechanical properties of the steel. Based on their experimental studies a new set of design rules was proposed for the shear strength of cold-formed steel beams. These design rules were adopted in AISI S100 (AISI, 2007) and AS/NZS 4600 (SA, 2005). However, they were developed by assuming simply supported web elements, thus the rigidity offered by the flange elements to the web was ignored and the post-buckling shear strength was also not considered. The shear strength design capacity ($V_v$) equations are provided next.

$$V_v = V_y = 0.6 f_{yw} d_1 t_w \qquad \text{for} \qquad \frac{d_1}{t_w} \leq \sqrt{\frac{E k_v}{f_{yw}}} \qquad (1)$$

$$V_v = V_i = 0.6 t_w^2 \sqrt{E k_v f_{yw}} \qquad \text{for} \qquad \sqrt{\frac{E k_v}{f_{yw}}} < \frac{d_1}{t_w} \leq 1.508 \sqrt{\frac{E k_v}{f_{yw}}} \qquad (2)$$

$$V_v = V_{cr} = \frac{k_v \pi^2 E t_w^3}{12 \left(1 - v^2\right) d_1} \quad \text{for} \qquad \frac{d_1}{t_w} > 1.508 \sqrt{\frac{E k_v}{f_{yw}}} \qquad (3)$$

where $V_y$ = Shear yield capacity, $V_i$ = Inelastic shear buckling capacity, $V_{cr}$ = Elastic shear bucking capacity, $d_1$ = depth of the flat portion of web measured along the plane of the web, $t_w$ = web thickness, $f_{yw}$ = web yield stress, $E$ = Young's modulus, $v$ = Poisson's ratio and $k_v$ is the elastic shear buckling coefficient, which is determined as follows.

For beams with transverse stiffeners

$$k_v = 5.34 + \frac{4}{\left(a/d_1\right)^2} \quad \text{for } \frac{a}{d_1} \geq 1 \qquad (4)$$

$$k_v = 4 + \frac{5.34}{\left(a/d_1\right)^2} \quad \text{for } \frac{a}{d_1} < 1 \qquad (5)$$

where 'a' = shear panel length and ($a/d_1$) = aspect ratio. $k_v$ is taken as 5.34 for unstiffened webs.

Pham and Hancock (2009) performed numerical analyses using an isoparametric spline finite strip method to study the elastic buckling behaviour of unlipped and lipped channel sections subject to shear. The numerical analyses showed that the flanges improved the shear buckling capacity of thin-walled channel sections. Further, it was shown that when there is inadequate lateral restraint for sections with narrow flanges, they can buckle prematurely in twisting and lateral buckling mode. Keerthan and Mahendran (2013) performed finite element analyses of LCB sections and proposed simplified design equations for the shear buckling coefficients, which include the effect of web-flange rigidity.

Pham and Hancock (2012) conducted both experimental and numerical studies to investigate the shear behaviour of high strength cold-formed steel LCB sections. Suitable design equations for the shear capacity of LCBs were then proposed in Pham and Hancock (2012). These shear design equations have been adopted in 2012 AISI S100 (AISI, 2012). These equations predict the shear capacities of LCBs which include their available post-buckling strength and the effect of additional fixity at the web-flange juncture.

Keerthan and Mahendran (2015 and 2011) investigated the shear behaviour of high strength cold-formed steel LCBs and LSBs using experimental and numerical studies. Based on their test and FEA results, they proposed appropriate design equations for the shear capacities of LCBs and LSBs (Equation 6 and 7). These design equations consider the effect of additional fixity at the web-flange juncture as well as post-buckling strength. In these equations the DSM based nominal shear capacity ($V_v$) is proposed based on $V_{cr}$ (elastic buckling capacity in shear) and $V_y$ (shear yield capacity).

$$V_v = V_y \qquad \text{for} \qquad \frac{d_1}{t_w} \le \sqrt{\frac{Ek_v}{f_{yw}}} \qquad (6)$$

$$V_V = \left[1 - 0.15\left(\frac{V_{cr}}{V_y}\right)^n\right]\left(\frac{V_{cr}}{V_y}\right)^n V_y \qquad \text{for} \qquad \frac{d_1}{t_w} > \sqrt{\frac{Ek_v}{f_{yw}}} \qquad (7)$$

where, n = 0.55 for LCBs and 0.50 for LSBs, $V_y$ and $V_{cr}$ are given by Equations 1 and 3, and $k_v$ is the enhanced elastic shear buckling coefficient of LCB and LSB sections and the equations to predict them are given in Keerthan and Mahendran (2010b and 2013).

Keerthan and Mahendran (2008) performed research on the elastic shear buckling behaviour of LiteSteel beams (LSBs) and proposed improved web shear buckling coefficient ($k_v$) considering the effect of web-flange rigidity. Their results showed that the presence of rigid hollow flanges increased the level of web to flange rigidity to 87% fixity level. In subsequent experimental and numerical studies by Keerthan and Mahendran (2010a and 2011) they developed appropriate shear capacity ($V_v$) equations by including the available post-buckling strength and the increased shear buckling coefficient ($k_v$). They also developed suitable DSM based design equations for the shear capacity of hollow flange channel beams (LSBs).

Web side plates are required to simulate the ideal simply supported end conditions during shear tests. Keerthan and Mahendran (2010a) investigated the effect of different sizes of the web side plates and having only one web side plate. They showed that the shorter web side plate heights as well as one side plate were not adequate to provide the required simply support conditions in the shear tests. Hence full web side plates were provided on both sides in their shear test set-up to simulate ideal simply supported conditions (not fixed conditions) for LiteSteel beams in shear. They were used at the supports and loading point to provide the required simply supported conditions, while also eliminating any web crippling and flange bearing failures. However, in LaBoube and Yu's (1978) test set-up, the LCB web elements appear to be not fully supported at the ends due to the use of only one web side plate with reduced number of bolt rows. Hence their tested LCBs might not have reached their full shear capacities due to premature failure (combined shear and web crippling failure). Pham and Hancock also reported that LaBoube and Yu's (1978) test specimens failed prematurely due to combined shear and web crippling.

Keerthan and Mahendran (2011) found that simply supported conditions are sufficient to develop post-buckling strength in web elements due to tension field action. They also found that web elements need to be fully supported at the ends to develop post-buckling strength in shear. Therefore a similar test set-up used in Keerthan and Mahendran (2010a) was considered in the shear tests of rivet fastened RHFCBs.

## 3. Shear Tests of Rivet Fastened RHFCBs

### 3.1. Test Specimens and Test Set-up

In this experimental study a series of 24 primarily shear tests of simply supported rivet fastened RHFCBs subjected to a mid-span load was conducted (see Figure 3 and Table 1). The RHFCB test sections were fabricated by connecting two rectangular hollow flanges to a web plate with rivets spaced at 100 mm. Due to fabrication limitations at the University Workshop, only one hollow flange of nominal dimensions, 51 mm flange width ($b_f$), 16 mm flange depth ($d_f$) and 20 mm lip length ($l_f$), was used in all the tests with varying web height and web and flange thicknesses. The hollow flange width to depth ratio was approximately three as for LSBs while a lip length of 20 mm was chosen to accommodate the required rivet.

Two rivet fastened RHFCB sections were bolted back to back using three 30 mm thick T-shaped stiffeners between them and twelve 10 mm full height web side plates on both sides, which were located at the end supports and the loading point in order to eliminate any torsional loading of test beams and possible web crippling and flange bearing failures. A 30 mm gap was included between the two rivet fastened RHFCB sections to allow the test beams to behave independently while remaining together to resist torsional effects. There is a possibility of flange distortion failure during the shear tests of rivet fastened RHFCBs. This failure mode was eliminated by restraining the flanges by using four small angle straps as shown in Figure 3. In order to simulate a primarily shear condition, relatively short test beams were selected based on suitable aspect ratios (shear span a/ clear web height $d_1$) of 1.0 and 1.5. Table 1 presents the details of the rivet fastened RHFCB test specimens used in this experimental study. It includes the measured web thicknesses ($t_w$), clear web heights ($d_1$) and yield stresses of the web elements ($f_{yw}$) of tested rivet fastened RHFCBs. As seen in Table 1, RHFCB section sizes are given as $d$x$b_f$x$t_f$x$t_w$, which are shown in Figure 2. Young's modulus (E) and Poisson's ratio were taken as 200 GPa and 0.3, respectively.

The rivet fastened RHFCB sections were loaded using the central T-shaped stiffener that was attached to the back to back test beams and the two web side plates with 4 M16 bolts at the mid-span loading point. The use of T-shaped stiffeners was important as they avoided bearing failures of the flanges. Such a loading method also eliminated eccentric loading and web crippling. Similar T-shaped stiffeners were also located at the supports, and were bolted to

the two rivet fastened RHFCBs and the two full web side plates on either side of the web element. It is assumed that such end support conditions enable the panel to be considered as fully supported at the end supports and the loading point in all the tests. Figure 3 shows the experimental set-up used in the shear tests of this research.

As seen in Figure 3 the test beam was provided with pinned supports at each end. The test beam was supported on round sections. The applied load at the mid-span of the test beam and associated test beam displacements were measured during the test until failure. Two laser displacement transducers were located on the test beam under the loading point and on the web panel to measure the vertical and lateral deflections, respectively, as seen in Figure 3.

### 3.2. Test Procedure

Two rivet fastened RHFCB were fabricated and their sizes, in particular, the clear web height ($d_1$) and web thickness ($t_w$), were measured as they are critical to the shear capacity calculations (Table 1). Test specimens were cut 50 mm longer than their required span in order to allow 25 mm overhang at each end of the test beam. Suitable bolt holes were then inserted at both the loading and support points to allow for effective connections at these points.

Shear span (a) was taken as the distance between the centres of inner bolts on the web side plates, and the required test specimen length was calculated based on the aspect ratio. For example, in the case of 200x51x1.15x1.15 RHFCBs with $d_1$ = 170 mm, shear span was 255 mm corresponding to an aspect ratio of 1.5. Hence the specimen length was 695 mm based on the spacing of bolts in the web side plates of 45 mm and the edge distance of outer bolts of 25 mm. Two rivet fastened RHFCBs were then assembled as back to back rivet fastened RHFCBs. The assembled pair of rivet fastened RHFCB sections was then positioned in the test rig and the three point loading was applied.

The clear height of web ($d_1$) of RHFCB is considered in the design instead of the depth of the flat portion of web measured along the plane of the web as defined in AS/NZS 4600 (SA, 2005) for cold-formed channel sections. This consideration is due to the following reasons.
   ❖ RHFCB has additional lips, which are likely to increase the shear capacity.

- ❖ RHFCB has two rectangular hollow flanges, which are likely to increase the shear yielding capacity by framing action.

- ❖ The corners between web and hollow flanges have short lips on both sides unlike in cold-formed channel sections.

- ❖ Buckling occurs within the clear height of web.

- ❖ Although the use of $d_1$ as the depth of the flat portion of web is conservative in estimating the shear yielding capacity, it is not safe in the case of elastic buckling.

At the start of the tests, a small load was applied on the test specimens to allow the entire test set-up to evenly settle on the bearings. The data acquisition system was then reset to zero before the actual loading was initiated. The loading rate of the testing machine's cross-head was kept at a constant rate of 0.7 mm/minute until the failure of the test specimens. Two laser displacement transducers were positioned and connected to the data acquisition system to measure the vertical and lateral deflections as shown in Figure 3.

## 3.3. Test Results

The full-scale shear tests were conducted to determine the actual ultimate shear capacities of rivet fastened RHFCB sections. The shear force on each beam was calculated based on the applied load (P) on the test specimens divided by four since each test set-up consisted of two RHFCB sections. Table 2 shows the shear capacities of rivet fastened RHFCB as obtained from this experimental study.

The load-deflection curve obtained from the shear test of 250x51x1.15x1.15 RHFCB (aspect ratio = 1.0) is shown in Figure 4. It can be seen that the web started to deflect out of plane at Point 1, indicating the elastic shear buckling load to be about 13.1 kN (applied load of 52.4 kN/4). At Point 2 the beam reached its ultimate shear capacity of 28.5 kN (applied load of 114 kN/4). These observations confirm that the slender rivet fastened RHFCBs have significant post-buckling capacity. Figures 5 (a) and (b) show the typical shear failure modes of 200x51x1.15x0.95 RHFCB with an aspect ratio (AR) of 1.0 and 250x51x1.15x0.95 RHFCB with an aspect ratio (AR) of 1.5, respectively while Figures 5 (c) and (d) show the shear failure modes of 250x51x1.15x0.95 RHFCB (AR = 1.0) and 200x51x0.95x0.95 RHFCB (AR = 1.0), respectively. These RHFCBs were made of a thinner web element (0.95 mm).

Figures 6 (a) to (c) show the shear failure modes of three RHFCBs with thicker web elements, 150x51x1.25x1.25 RHFCB 2000x51x1.25x1.25 RHFCB and 250x51x1.25x1.25 RHFCB (AR = 1.5), respectively. Figure 7 (a) shows the plot for applied load versus lateral deflection for 200x51x1.25x1.25 RHFCB with an aspect ratio of 1.0, and confirms the presence of significant reserve capacity beyond elastic buckling for RHFCBs. Keerthan and Mahendran (2011) found that slender welded LSB web panels do not collapse when elastic buckling stress is reached and still have considerable post-buckling strength. Figure 7 (b) shows the mechanics of rivet fastened RHFCB web panel post-buckling behaviour in shear. It shows that there is no separation between the two flange lips and the web of RHFCB in the elastic buckling and ultimate failure stages (see Figure 7 (b)) with a small separation in the post-ultimate failure stage.

All the RHFCB test specimens were rivet fastened at 100 mm spacing as seen in Figures 5 to 7. This spacing was chosen based on preliminary shear and bending tests of RHFCBs (Siahaan et al., 2014a,b). The shear tests conducted in this study did not show any unacceptable separation between the two flange lips and the web of RHFCB test specimens (see Figure 7). There was noticeable separation of flange lips and web element only after the ultimate load was reached with test specimens retaining the torsional rigidity provided by the hollow flanges. The lack of continuity along the web to flange juncture did not appear to cause any major changes to the expected shear buckling and failure modes as seen in Figures 5 to 7. Their shear failure modes were similar to those observed for welded RHFCBs (LSBs) and included tension field action (Keerthan and Mahendran, 2010a and 2010b). Shear test results also showed that there were no rivet fastener failures. However, the effect of rivet spacing should be further investigated using numerical and experimental studies.

The shear tests were carried out on relatively short beams with aspect ratios of 1.0 and 1.5. Although these test specimens were assumed to be subjected to pure shear due to their shorter spans and lower aspect ratios, the beams were also subjected to a bending moment. However, it is safe to assume that this bending moment did not affect the shear capacities computed from these tests because, the ratio of the applied moment ($M^*$) to the section moment capacity ($\phi M_s$) is less than 0.75 based on the design rules of AS 4100 (SA, 1998) for combined bending and shear actions. This was confirmed previously by Keerthan and Mahendran

(2014a and 2014b), in which they found that this ratio for welded hollow flange channel beams (LSBs) is less than 0.65. However, test specimens 21 to 24 failed in combined bending and shear actions. Thus, only the test specimens which failed under primarily shear action were considered in the following sections. Figures 8 (a) and (b) show the combined bending and shear failure modes of 150x51x1.15x1.50 RHFCB with an aspect ratio of 1.0 and 150×51×1.15×1.15 RHFCB with an aspect ratio of 1.5, respectively. Test Specimens 21 to 24 failed primarily due to bending with only minor evidence of shear failure. Local buckling/yielding of the compression flange was much more pronounced in these specimens, which failed primarily by bending at mid-span.

Test specimens with aspect ratio of 1.0 generally failed in primarily shear. However Test specimens 21 and 22 (AR =1.0) failed in the combined bending and shear failure mode. In Test specimens 21 and 22, the web thicknesses and yield strengths were 1.5 mm and 545 MPa, and 1.9 mm and 480 MPa, ie. higher than the flange thickness and yield strength of 1.1 mm and 310 MPa. Hence these test specimens had a lower section moment capacity in relation to their shear capacity, and thus failed in the combined bending and shear failure mode.

The shear capacities from the experimental study are compared with the predictions based on the current cold-formed steel design standard AS/NZS 4600 (SA, 2005) (Table 2). The mean value of the ratios of shear capacities from test results and AS/NZS 4600 design rules is 2.58 with a coefficient of variation of 0.441. This comparison clearly shows that the shear capacities are significantly under-estimated by the current AS/NZS 4600 design rules. This is because they do not include the post-buckling strength observed in the shear tests and the effect of increased fixity at the web to flange juncture of rivet fastened RHFCBs despite the lack of continuous fastening/welding. Hence improved shear capacity equations were proposed in the following section based on the current shear capacity design equations in AISI S100 (AISI, 2012) and experimental results.

## 4. Proposed Equations for the Shear Capacity of Rivet Fastened RHFCBs

Keerthan and Mahendran (2010a and 2011) developed new shear strength equations for welded LSBs based on the current shear strength design equations in AISI S100 (AISI, 2007), experimental and finite element analysis results. Similar equations can be developed for rivet

fastened RHFCBs subject to primarily shear action. Eqs. (8) to (10) present the proposed shear strength equations which include the available post-buckling strength and the additional fixity at the web-flange juncture in the rivet fastened RHFCBs tested in this study (100 mm rivet spacing).

Equations 9 and 10 include the experimentally observed post-buckling strength in rivet fastened RHFCBs and the additional fixity at the web-flange juncture. In these equations, a post-buckling coefficient of 0.45 is introduced to include the available post-buckling strength in rivet fastened RHFCBs. They also include the effects of additional fixity at the web-flange juncture of RHFCBs. This effect is included using an increased shear buckling coefficient ($k_{RHFCB}$). For this purpose, finite element elastic buckling analyses of rivet fasted RHFCBs were performed with a 100 mm rivet spacing as used in the shear tests. Finite element models of RHFCBs in shear were developed using the same principles described in Keerthan and Mahendran (2011) for welded LSBs. In these models the rivets connecting the hollow flange lips to the web were not explicitly simulated. Instead they were simulated using perfect Tie MPCs as the test results showed that there were no rivet fastener failures, which makes all active degrees of freedom equal on both sides of the connection. Equation 11 presents the proposed equation for $k_{RHFCB}$ based on the elastic shear buckling loads of RHFCBs obtained from finite element analyses. For the welded LSBs, the coefficient in Equation 11 was 0.87, indicating the benefit of web-flange continuity. The use of this coefficient as 0.80 is considered to provide safer predictions for rivet fastened RHFCBs. It also implies that the effect of rivet spacing on elastic shear buckling strength and thus on ultimate shear strength of RHFCBs is small. However, further finite element analyses will be carried out to investigate the effect of rivet spacing on the shear buckling coefficient of rivet fastened RHFCBs.

$$V_v = V_y \qquad \text{for} \qquad \frac{d_1}{t_w} \leq \sqrt{\frac{Ek_{RHFCB}}{f_{yw}}} \qquad \text{(Shear yielding)} \qquad (8)$$

$$V_v = V_i + 0.45\left(V_y - V_i\right) \quad \sqrt{\frac{Ek_{RHFCB}}{f_{yw}}} < \frac{d_1}{t_w} \leq 1.508\sqrt{\frac{Ek_{RHFCB}}{f_{yw}}} \quad \text{(Inelastic shear buckling)} \qquad (9)$$

$$V_v = V_{cr} + 0.45\left(V_y - V_{cr}\right) \quad \frac{d_1}{t_w} > 1.508\sqrt{\frac{Ek_{RHFCB}}{f_{yw}}} \quad \text{(Elastic shear buckling)} \qquad (10)$$

where, $V_y$ (shear yield capacity), $V_i$ ( inelastic shear buckling capacity ) and $V_{cr}$ (Elastic shear buckling capacity ) are given by Eqs. 1 to 3, respectively.

For rivet fastened RHFCBs    $k_{RHFCB} = k_{ss} + 0.80(k_{sf} - k_{ss})$ (11)

$$k_{sf} = \frac{5.34}{(a/d_1)^2} + \frac{2.31}{(a/d_1)} - 3.44 + 8.39(a/d_1) \quad \text{for} \quad \frac{a}{d_1} < 1$$ (12)

$$k_{sf} = 8.98 + \frac{5.61}{(a/d_1)^2} - \frac{1.99}{(a/d_1)^3} \quad \text{for} \quad \frac{a}{d_1} \geq 1$$ (13)

where $k_{ss}$ and $k_{sf}$ are the shear buckling coefficients of plates with simple-simple and simple-fixed boundary conditions, and $k_{ss}$ is given by Eqs. 4 and 5.

The AS/NZS 4600 (SA, 2005) design equations do not include the post-buckling strength in shear, thus the design shear stress in the web is limited by the elastic buckling capacity. However, Keerthan and Mahendran's (2010a) experimental studies have shown that post-buckling shear strength is present in LSBs, which can be included in their design equations. Experimental results discussed in Section 3 have also shown that significant reserve shear strength beyond elastic buckling is present in rivet fastened RHFCBs. Therefore Equations 8 to 10 can be used to predict the accurate shear capacity of rivet fastened RHFCBs by considering post-buckling shear strength and the web-flange fixity using a post-buckling coefficient of 0.45 and a higher buckling coefficient (Equation 11), respectively.

The recently developed direct strength method (DSM) is superior to the traditional effective width method that has been adopted as an alternative design procedure in AISI S100 (AISI, 2007) and AS/NZS 4600 (SA, 2005). Hence the proposed Equations (8) to (10) are reorganized in the DSM format and are given as Equations (14) to (16).  In these equations, the required shear slenderness ($\lambda$) was calculated using Equation 17. Table 3 compares the shear test capacities with the corresponding shear capacities predicted by Equations 14 to 16. Comparison of test capacities with predicted capacities from Equations 14 to 16 show a good agreement with a mean of 1.06 and a COV of 0.087 unlike in the case of AS/NZS 4600 design equations (see Table 2).

**Direct Strength Method**

$$\frac{V_v}{V_y} = 1 \qquad \text{for} \qquad \lambda \leq 0.815$$ (14)

$$\frac{V_v}{V_y} = \frac{0.815}{\lambda} + 0.45\left(1 - \frac{0.815}{\lambda}\right) \qquad \text{for} \qquad 0.815 < \lambda \leq 1.23$$ (15)

$$\frac{V_v}{V_y} = \frac{1}{\lambda^2} + 0.45\left(1 - \frac{1}{\lambda^2}\right) \qquad \text{for} \qquad \lambda > 1.23 \qquad (16)$$

where

$$\lambda = \sqrt{\left(\frac{V_y}{V_{cr}}\right)} = 0.815\left(\frac{d_1}{t_w}\right)\sqrt{\left(\frac{f_{yw}}{Ek_{RHFCB}}\right)} \qquad (17)$$

New design equations were also proposed for the shear strength of rivet fastened RHFCBs in a similar manner to those of the section moment capacity of beams subject to local buckling (Equations 18 and 19) using our experimental results. These equations are based on the DSM format. As in hot-rolled I-sections, only two regions based on shear yielding, and elastic and inelastic shear buckling, were considered. In these equations, a power coefficient of 0.3 was used based on the experimental results of rivet fastened RHFCBs from this study.

$$V_v = V_y \quad \text{for} \qquad \frac{d_1}{t_w} \leq 0.86\sqrt{\frac{Ek_{RHFCB}}{f_{yw}}} \qquad \text{(Shear yielding)} \qquad (18)$$

$$V_v = \left[1 - 0.15\left(\frac{V_{cr}}{V_y}\right)^{0.30}\right]\left(\frac{V_{cr}}{V_y}\right)^{0.30} V_y \quad \text{for} \quad \frac{d_1}{t_w} > 0.86\sqrt{\frac{Ek_{RHFCB}}{f_{yw}}}$$

(Elastic and inelastic shear buckling) $\qquad (19)$

Comparison of test capacities with predicted capacities from the DSM equations (Equations 18 and 19) in Table 3 shows a good agreement with a mean of 1.08 and a COV of 0.086 unlike in the case of AS/NZS 4600 design equations (see Table 2).

Experimental ultimate shear capacity results were also calculated based on the DSM format and compared with the proposed DSM based design equations. The required $V_y$, $V_{cr}$ and $\lambda$ values of test specimens are provided in Table 4. Figure 9 shows the non-dimensional shear capacity curves for rivet fastened RHFCBs and the experimental results. In this figure, the shear capacities are plotted in a non-dimensional format of $V_v/V_y$ versus $\lambda$, where $\lambda$ is $(V_y/V_{cr})^{0.5}$. It can be seen that shear design equations without post-buckling strength (Equations 1 to 3) are significantly underestimating the shear capacities of rivet fastened RHFCBs. However, Equations (14) to (16) and (18) and (19) safely predict the shear

capacities while also including the available post-buckling strength and additional fixity at the web-flange juncture reasonably well (see Figure 9).

In order to investigate the effect of flange thickness to web thickness ($t_f/t_w$) ratio on the ultimate shear capacities of rivet fastened RHFCBs, it was varied from 1.0 to 1.6 in the shear tests as seen in Table 2. However, when it was increased from 1.2 to 1.6 in Tests 19 and 20, the shear capacities increased considerably more than in other tests with smaller $t_f/t_w$ ratios. Hence the design equations proposed in this section were limited to $t_f/t_w$ ratio of 1.2, i.e., Tests 19 and 20 were not considered in developing the design equations (Equations 14 to 16, 18 and 19). The proposed design rules are conservative for Tests 19 and 20 as seen in the comparisons in Tables 3 and 4. Detailed numerical studies will be conducted to investigate the effect of $t_f/t_w$ ratio on the ultimate shear capacities of rivet fastened RHFCBs. However, the proposed design equations can be used in designs as their predictions are conservative for higher $t_f/t_w$ ratios.

Figure 10 shows the non-dimensional shear capacity curves for rivet fastened RHFCBs and the experimental results. The ultimate shear capacities of welded LiteSteel beams from experiments were also included in Figure 10. The level of fixity along the web to flange juncture was similar for both welded and rivet fastened beams based on the elastic buckling finite element analyses. These analyses showed a small reduction in fixity for rivet fastened RHFCBs as reflected by its shear buckling coefficients $k_{RHFCB}$ (0.80 versus 0.87 in Equation 11). However, Figure 10 shows that the shear capacities of rivet fastened RHFCB are slightly higher than the shear capacities of LSBs, which is likely to be due to the contribution from the additional lips in rivet fastened RHFCBs.

When the flange thickness to web thickness ($t_f/t_w$) ratio was increased from 1.2 to 1.6 in Tests 19 and 20, the shear capacities increased considerably more than in other tests with smaller $t_f/t_w$ ratios (more than 30% increment in shear capacity). One of the main contributors could be the two additional thicker lips. In the rivet fastened RHFCBs, shear buckling is likely to occur within the top and bottom rivet levels. Therefore the effective clear height ($d_{eff}$) will be less than clear height of web ($d_1$). This can also lead to the increased in shear capacity of RHFCBs. Further detailed numerical studies will be conducted to extend the available shear capacity data for rivet fastened RHFCBs and to confirm the accuracy of the developed shear capacity equations.

Figure 11 shows the shear failure mechanism of rivet fastened RHFCBs. There is small separation between the two flange lips and the web of RHFCB test specimens in the diagonal compression region and no separation between the two flange lips and the web of RHFCB test specimens in the diagonal tension region as shown in Figure 11 (Post-Failure Stage). Post-buckling strength of rivet fastened RHFCBs mainly depends on the tension field action (TFA). It will not be reduced significantly due to the small separation in the diagonal compression region in the post-failure stage.

## 5. Conclusions

This paper has presented the details of an experimental investigation into the shear behaviour and capacity of rivet fastened rectangular hollow flange channel beams (RHFCBs). The ultimate shear capacities measured from the tests showed that AS/NZS 4600 (SA, 2005) design equations are very conservative for the shear design of rivet fastened RHFCBs. Rivet fastened RHFCBs exhibited considerably enhanced web shear buckling and post-buckling capacity when subjected to shear. New shear capacity equations were proposed based on the current shear strength design equations in AISI S100 (2012) and experimental results to incorporate these enhancements in shear capacity. Suitable shear design rules were also developed under the direct strength method format. This experimental study was limited to 100 mm rivet spacing and hence further research is currently under way to investigate the effect of different rivet spacings and flange to web thickness ratios on the shear capacities of RHFCBs.

**References**

American Iron and Steel Institute (AISI) (2007), North American Specification for the Design of Cold-formed Steel Structural Members, AISI S100, Washington, DC, USA.

American Iron and Steel Institute (AISI) (2012), North American Specification for the Design of Cold-formed Steel Structural Members, AISI S100, Washington, DC, USA.

Anapayan, T., Mahendran, M. and Mahaarachchi, D. (2011), Section Moment Capacity Tests of LiteSteel Beams. Thin-Walled Structures, Vol. 49, pp. 502-512.

Anapayan, T. and Mahendran, M. (2012a), Improved Design Rules for Hollow Flange Sections Subject to Lateral Distortional Buckling. Thin-Walled Structures, Vol. 50, pp. 128-140.

Anapayan, T. and Mahendran, M. (2012b), Numerical Modelling and Design of LiteSteel Beams Subject to Lateral Buckling, Journal of Constructional Steel Research, Vol.70, pp.51-64.

Keerthan, P. and Mahendran, M. (2008), Shear Behaviour of LiteSteel Beams, Proceedings of the 5th International Conference on Thin-Walled Structures, Brisbane, Australia, pp.411-418.

Keerthan, P. and Mahendran, M. (2010a), Experimental Studies on the Shear Behaviour and Strength of LiteSteel Beams, Engineering Structures, Vol 32, pp. 3235-3247.

Keerthan, P. and Mahendran, M. (2010b), Elastic Shear Buckling Characteristics of LiteSteel Beams, Journal of Constructional Steel Research, Vol. 66, pp. 1309-1319.

Keerthan, P. and Mahendran, M. (2011), New Design Rules for the Shear Strength of LiteSteel Beams, Journal of Constructional Steel Research, Vol. 67, pp. 1050–1063.

Keerthan, P. and Mahendran, M. (2013), Shear Buckling Characteristics of Cold-formed Steel Channel Beams, International Journal of Steel Structures, Vol. 13, pp. 385–399.

Keerthan, P., Hughes, D. and Mahendran, M. (2014a), Experimental Studies of Hollow Flange Channel Beams Subject to Combined Shear and Bending Actions, Thin-Walled Structures, Vol. 77, pp. 129–140.

Keerthan, P., Mahendran, M. and Hughes, D. (2014b), Numerical Studies and Design of Hollow Flange Channel Beams Subject to Combined Bending and Shear Actions, Engineering Structures, Vol. 75, pp. 197–212.

Keerthan, P., Mahendran, M. and Steau, E. (2014c), Experimental Study of Web Crippling Behaviour of Hollow Flange Channel Beams under Two Flange Load Cases, Thin-Walled Structures, Vol. 85, pp. 207-219.

Keerthan, P. and Mahendran, M. (2015), Experimental Investigation and Design of Lipped Channel Beams in Shear. Thin-Walled Structures, Vol. 86, pp. 174-184.

LaBoube, R.A. and Yu, W.W. (1978), Cold-formed Steel Beam Webs Subjected Primarily to Shear, Research Report, American Iron and Steel Institute, University of Missouri-Rolla, Rolla, USA.

OneSteel Australian Tube Mills, (OATM) (2008), Design of LiteSteel Beams, Brisbane, Australia.

Pham, C.H. and Hancock, G.J. (2009), Shear Buckling of Thin-Walled Channel Sections, Journal of Constructional Steel Research, Vol 65, pp. 578-585.

Pham, C.H. and Hancock, G.J. (2012), Direct Strength Design of Cold-Formed C-Sections for Shear and Combined Actions, Journal of Structural Engineering, American Society of Civil Engineers, Vol. 138, pp. 759–768.

Siahaan, R., Keerthan, P. and Mahendran, M. (2014a), Section Moment Capacity Tests of Rivet Fastened Rectangular Hollow Flange Channel Beams, Proc. of 22nd International Specialty Conference on Cold-Formed Steel Structures, St Louis, Missouri, USA, pp. 277-294.

Siahaan, R., Keerthan, P. and Maendran, M. (2014b), Numerical Studies of Rivet-fastened Rectangular Hollow Flange Channel Beams, Proc. of 22nd International Specialty Conference on Cold-Formed Steel Structures, St Louis, Missouri, USA, pp. 259-276.

Seo, J. K. and Mahendran, M. (2011), Plastic Bending Behaviour and Section Moment Capacities of Mono-symmetric LiteSteel Beams with Web Openings, Thin-Walled Structures, Vol. 49, pp. 513-522.

Seo, J.K, and Mahendran, M., 2012, Member Moment Capacities of Mono-symmetric LiteSteel Beam Floor Joists with Web Openings, Journal of Constructional Steel Research, Vol. 70, pp. 153-166.

Standards Australia (1998). Australian Standard AS 4100 Steel Structures, Sydney, Australia.
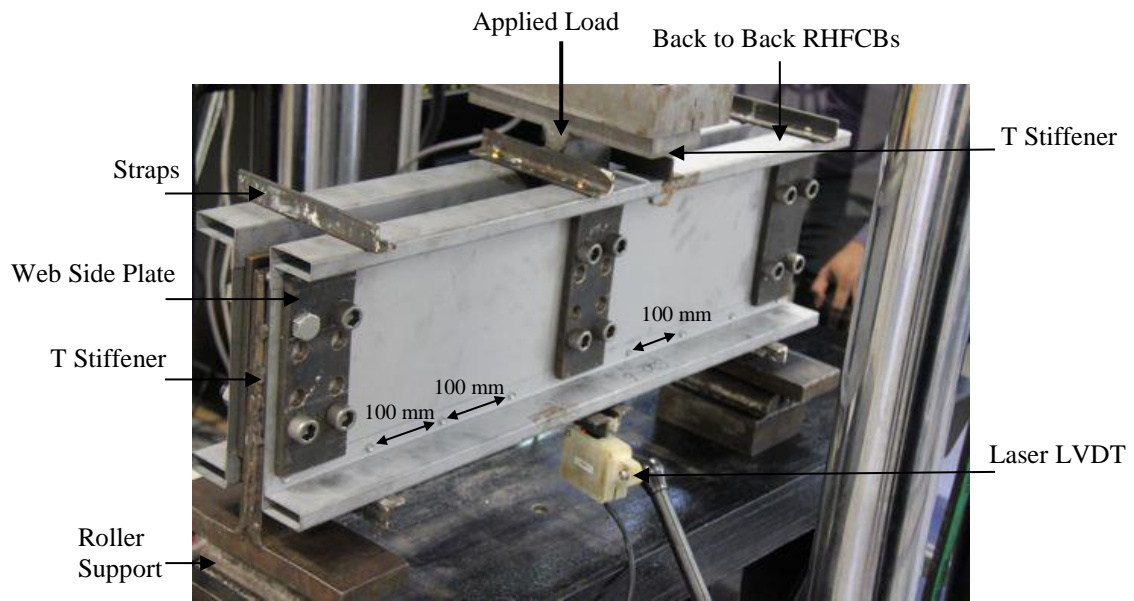
Standards Australia/Standards New Zealand (2005), Australia/New Zealand Standard AS/NZS4600 Cold-Formed Steel Structures, Sydney, Australia.
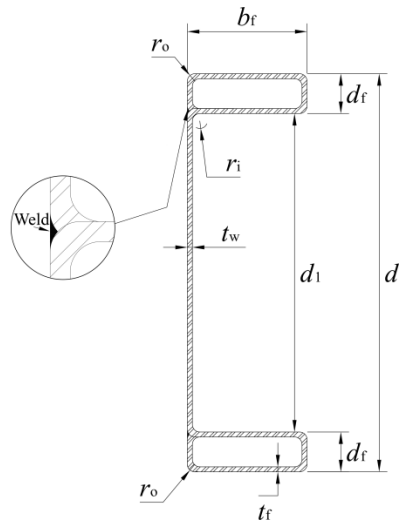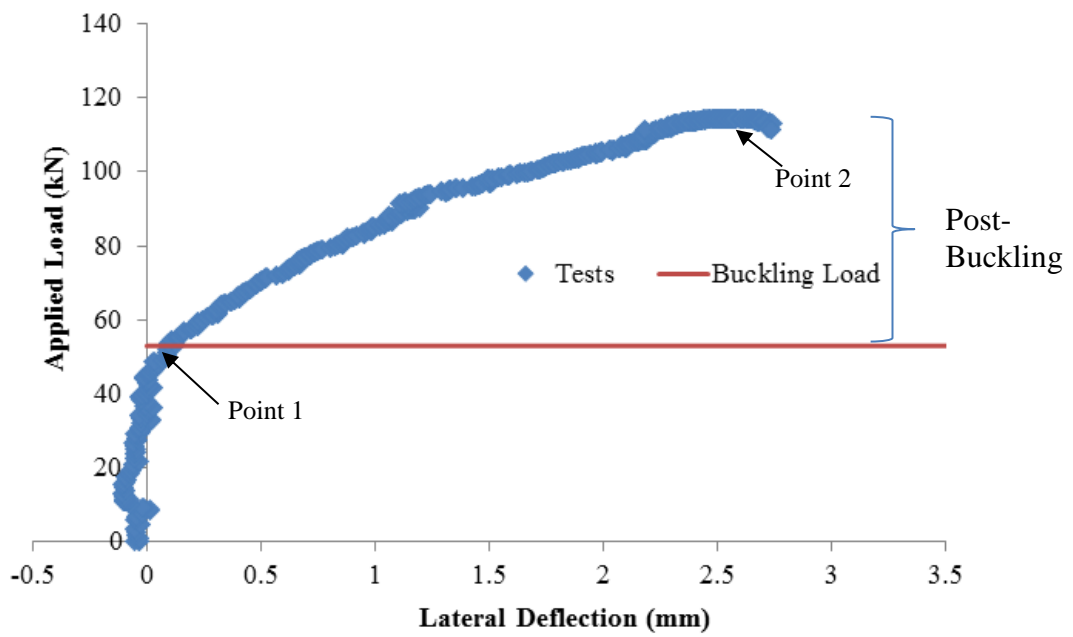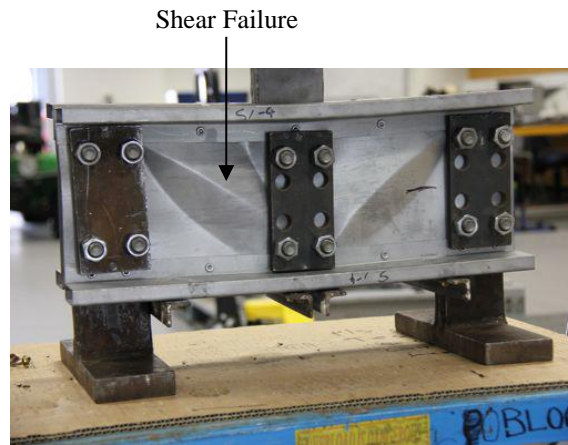
**Figure 1:  LiteSteel Beam (OATM, 2008)**
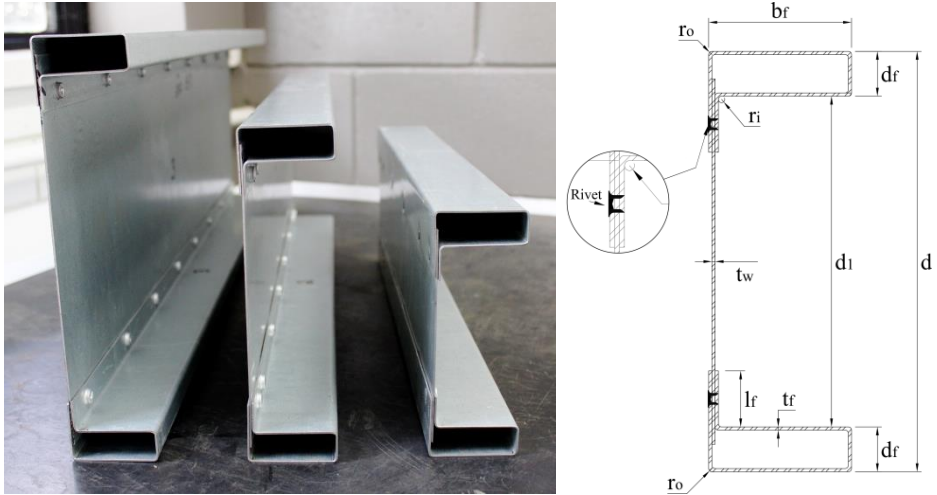
**Figure 2: Rivet Fastened Rectangular Hollow Flange Channel Beam (RHFCB)**
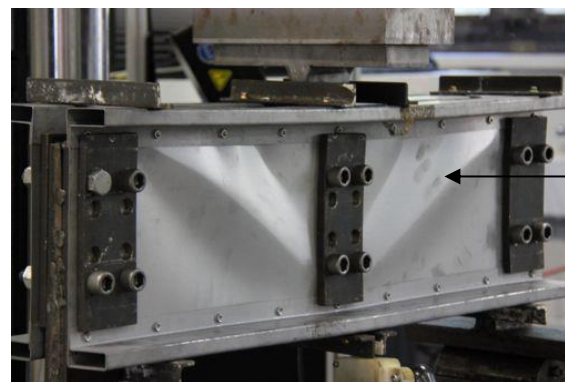
**Figure 3:  Shear Test Set-up**

**Figure 4: Plot of Applied Load versus Lateral Deflection**
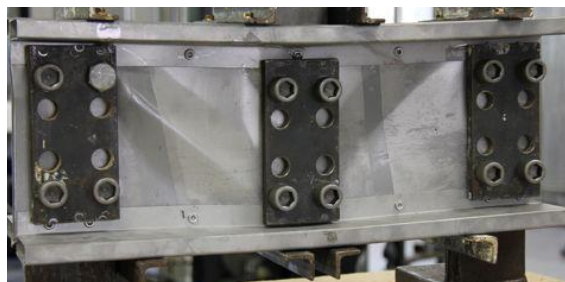**(250x51x 1.15x1.15 RHFCB, Aspect Ratio = 1.0)**

Shear Failure



(a) 200x51x1.15x0.95 RHFCB (Test 5, AR of 1.0)



Shear Failure

(b) 250x51x1.15x0.95 RHFCB (Test 15, AR of 1.5)



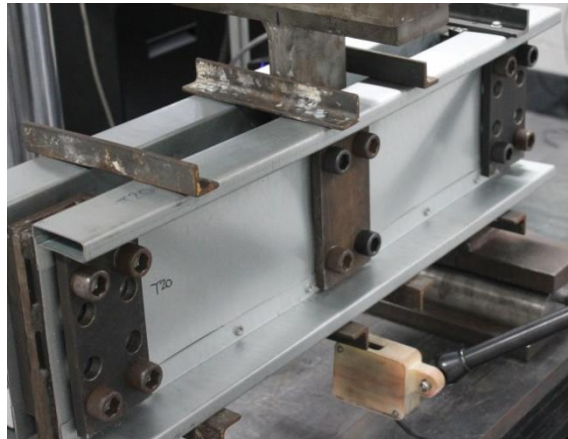(c) 250x51x1.15x0.95 RHFCB (Test 7, AR of 1.0)



(d) 200x51x0.95x0.95 RHFCB (Test 3, AR of 1.0)

**Figure 5: Shear Failure Modes of Rivet Fastened RHFCBs with Thinner Web Elements**

(a)  150x51x1.25x1.25 RHFCB


(b)  200x51x1.25x1.25 RHFCB
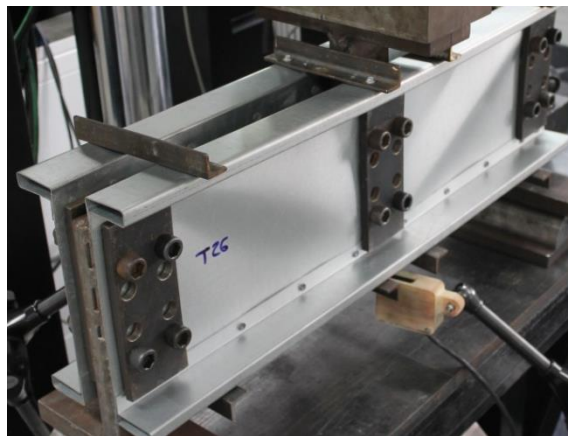

(c)  250x51x1.25x1.25 RHFCB

**Figure 6: Shear Failure Modes of Rivet Fastened RHFCBs with Thicker Web Elements (AR = 1.5)**
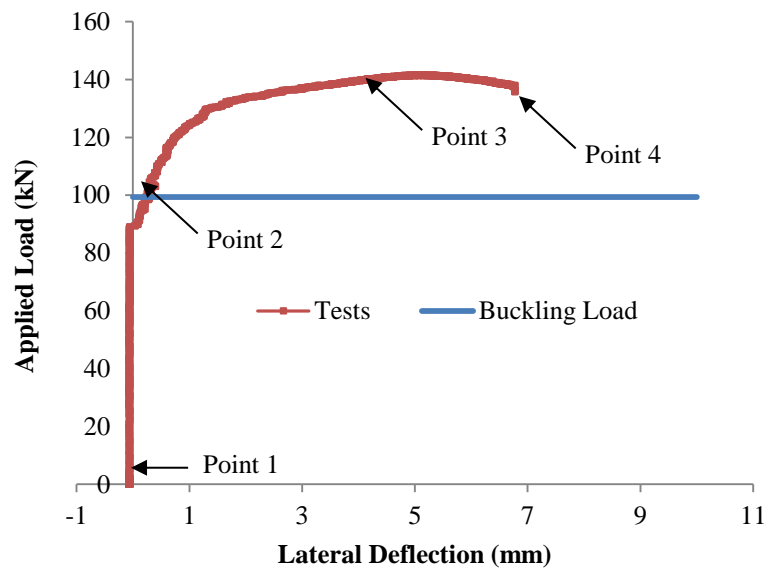
(a) Applied Load versus Lateral Deflection



(1) Point 1 (Initial Stage)
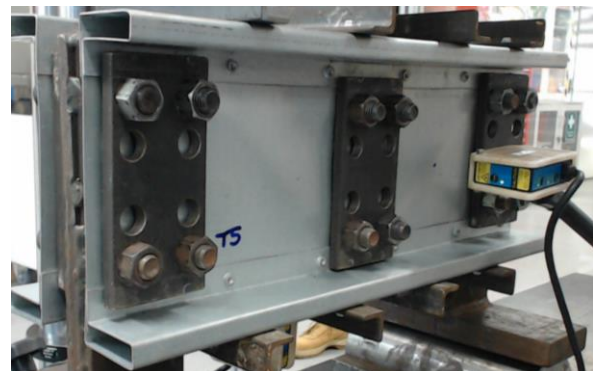


(2) Point 2 (Elastic Buckling Stage)



No Separation in compression region

(3) Point 3 (Ultimate Failure Stage)



Small Separation in compression region

(4) Point 4 (Post-Ultimate Stage)

(b) Shear Failure Mode

**Figure 7: Mechanics of RHFCB Web Panel Post-buckling Behaviour in Shear**
**200x51x1.25x1.25 RHFCB (AR =1.0)**

7
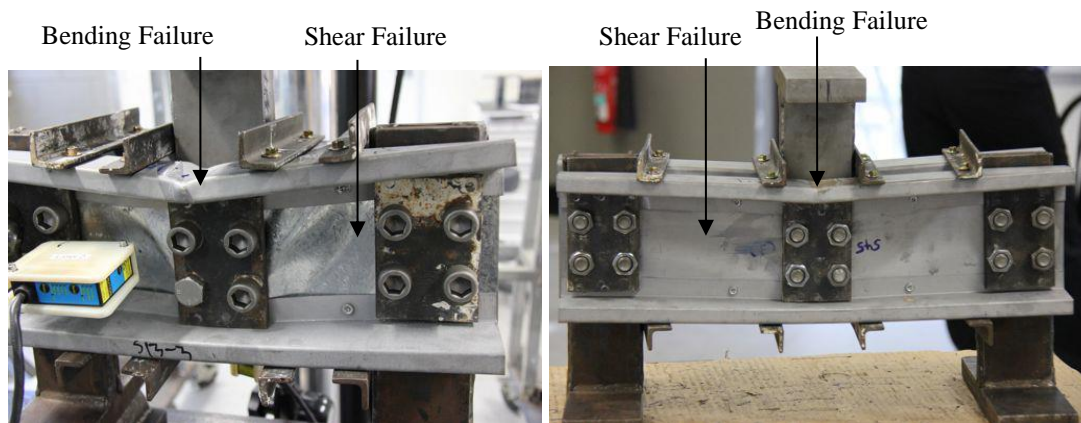
(a) 150x51x1.15x1.50 RHFCB (Test 21, AR of 1.0)      (b) 150x51x1.15x1.15 RHFCB (Test 23, AR of 1.5)

**Figure 8: Combined Bending and Shear Failure Modes of Rivet Fastened RHFCBs**
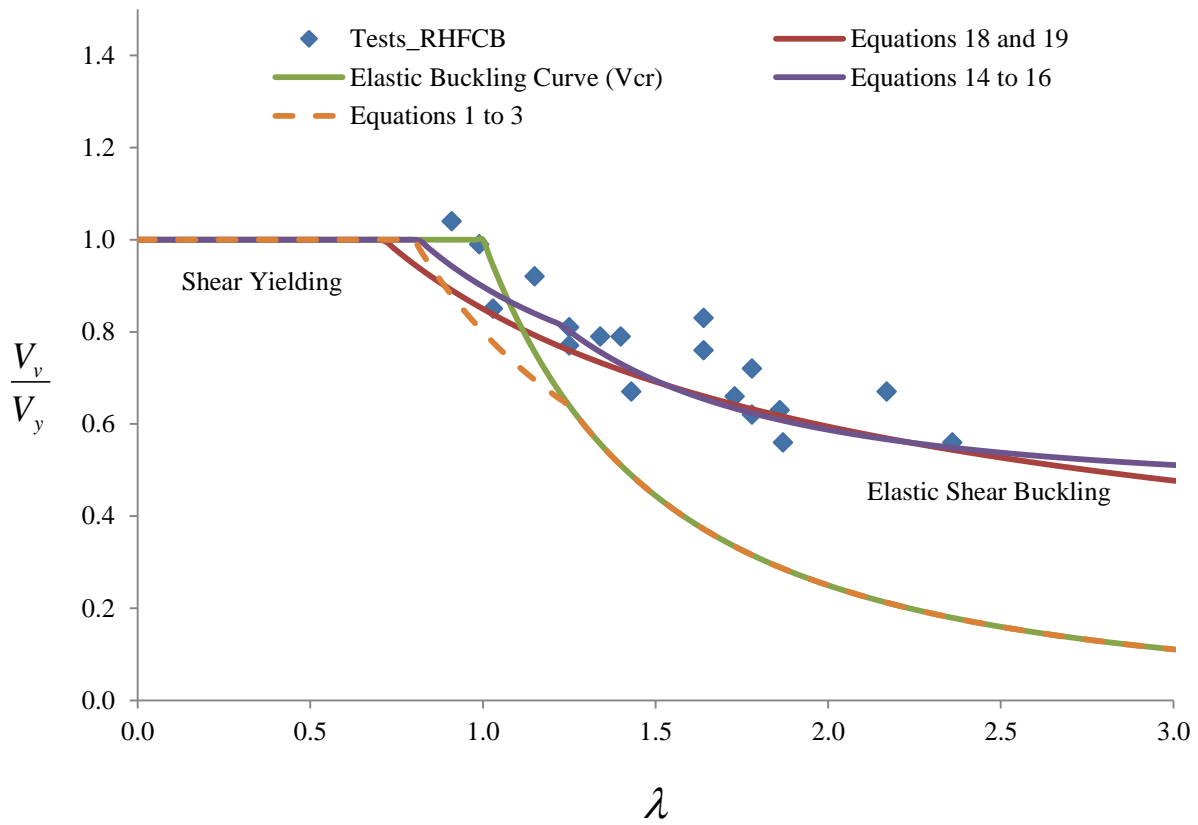
**Figure 9: Comparison of Experimental Shear Capacities of Rivet Fastened RHFCBs with DSM based Design Equations**
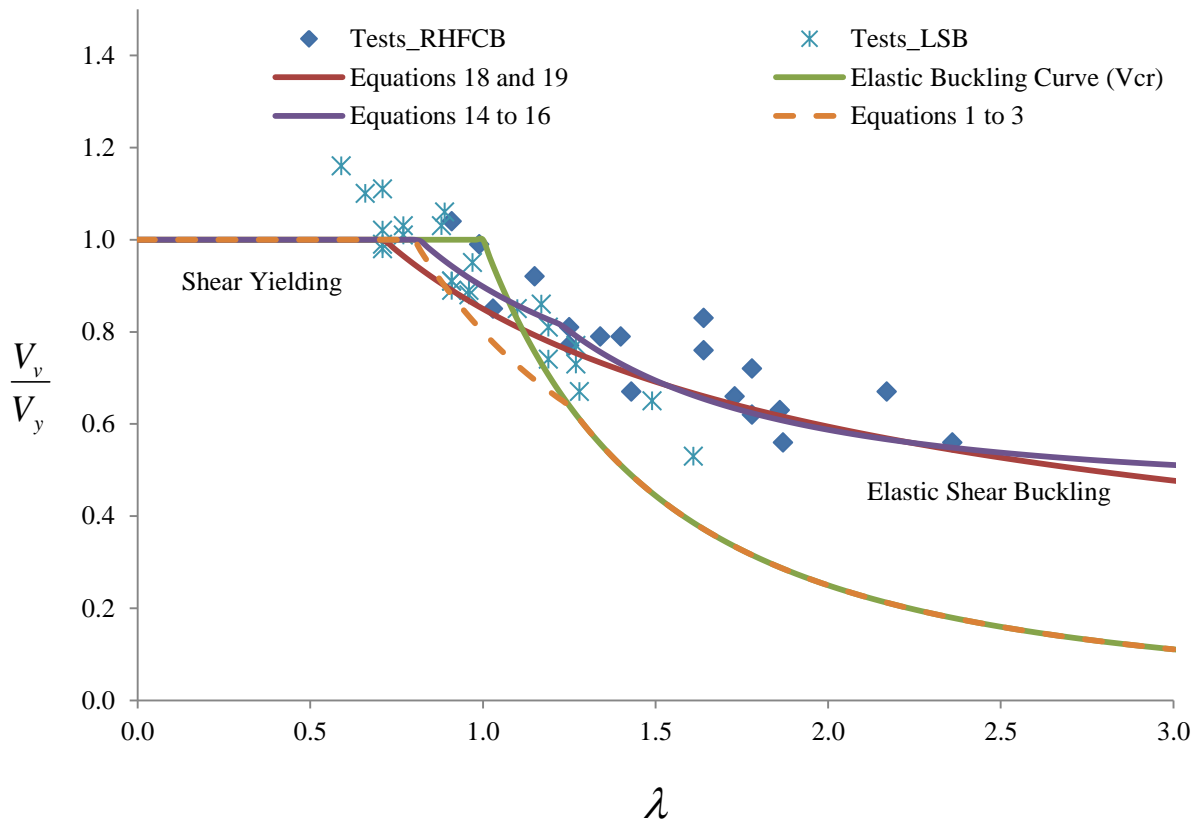
**Figure 10: Comparison of Experimental Shear Capacities of Rivet Fastened RHFCBs and LSBs with DSM based Design Equations**

Separation in Compression Region in the Post-Failure Stage

Tension Field Action (TFA)

Top flange in compression

Compression

Tension

Tension

Compression

Bottom flange in tension
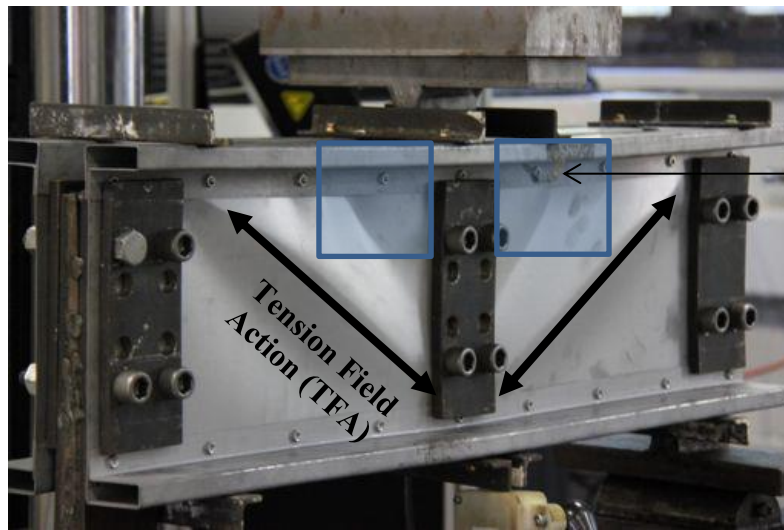
**Figure 11: Shear Failure Mechanism of Rivet Fastened RHFCBs**

**Table 1: Details of Rivet Fastened RHFCB Specimens**

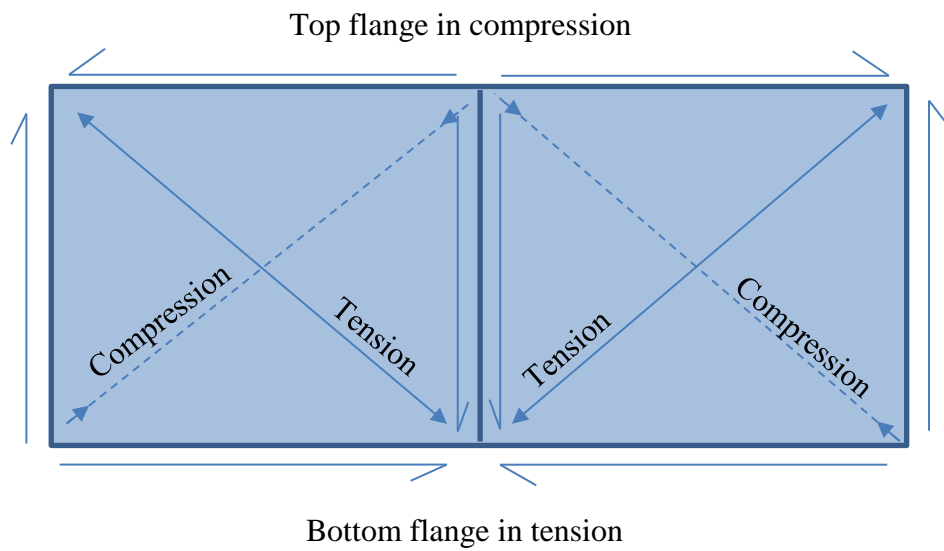| Test No. | RHFCB Section $(d \times b_f \times t_f \times t_w)$ | $d_1$ (mm) | $t_w$ (mm) | $f_y$ (MPa) | $a/d_1$ |
|---|---|---|---|---|---|
| 1 | 150x51x0.95x0.95 | 117 | 0.91 | 290 | 1.0 |
| 2 | 150x51x1.15x1.15 | 117 | 1.10 | 310 | 1.0 |
| 3 | 200x51x0.95x0.95 | 166 | 0.91 | 290 | 1.0 |
| 4 | 200x51x1.15x1.15 | 166 | 1.10 | 310 | 1.0 |
| 5 | 200x51x1.15x0.95 | 166 | 0.91 | 290 | 1.0 |
| 6 | 250x51x1.15x1.15 | 220 | 1.10 | 310 | 1.0 |
| 7 | 250x51x1.15x0.95 | 220 | 0.91 | 290 | 1.0 |
| 8 | 150x51x1.25x1.25 | 115 | 1.25 | 352 | 1.0 |
| 9 | 200x51x1.25x1.25 | 170 | 1.25 | 352 | 1.0 |
| 10 | 250x51x1.25x1.25 | 219 | 1.25 | 352 | 1.0 |
| 11 | 150x51x0.95x0.95 | 117 | 0.91 | 290 | 1.5 |
| 12 | 150x51x1.15x0.95 | 117 | 0.91 | 290 | 1.5 |
| 13 | 200x51x0.95x0.95 | 166 | 0.91 | 290 | 1.5 |
| 14 | 200x51x1.15x0.95 | 166 | 0.91 | 290 | 1.5 |
| 15 | 250x51x1.15x0.95 | 220 | 0.91 | 290 | 1.5 |
| 16 | 150x51x1.25x1.25 | 120 | 1.25 | 352 | 1.5 |
| 17 | 200x51x1.25x1.25 | 167 | 1.25 | 352 | 1.5 |
| 18 | 250x51x1.25x1.25 | 217 | 1.25 | 352 | 1.5 |
| 19 | 150x51x1.15x0.70 | 117 | 0.71 | 303 | 1.5 |
| 20 | 200x51x1.15x0.70 | 166 | 0.71 | 303 | 1.5 |
| 21 | 150x51x1.15x1.50 | 117 | 1.55 | 545 | 1.0 |
| 22 | 150x51x1.15x1.90 | 117 | 1.91 | 480 | 1.0 |
| 23 | 150x51x1.15x1.15 | 117 | 1.10 | 310 | 1.5 |
| 24 | 250x51x1.15x1.15 | 220 | 1.10 | 310 | 1.5 |

Note: d = overall height, $b_f$ = flange width (51 mm), $d_f$ = flange depth (16 mm), $l_f$ = lip length (20 mm), $t_f$ = flange thickness, $t_w$ = web thickness, a = shear span, $d_1$ = clear height of web, $f_y$ = web yield stress.

**Table 2: Shear Capacities of Rivet Fastened RHFCBs**

| Test No. | RHFCB Section ($d \times b_f \times t_f \times t_w$) | $a/d_1$ | $t_f/t_w$ | Shear Capacity (kN) | | Test/ AS/NZS 4600 |
| --- | --- | --- | --- | --- | --- | --- |
| | | | | Test | AS/NZS 4600 | |
| 1 | 150x51x0.95x0.95 | 1.0 | 1.0 | 17.00 | 10.89 | 1.56 |
| 2 | 150x51x1.15x1.15 | 1.0 | 1.0 | 23.75 | 18.64 | 1.27 |
| 3 | 200x51x0.95x0.95 | 1.0 | 1.0 | 20.08 | 7.67 | 2.62 |
| 4 | 200x51x1.15x1.15 | 1.0 | 1.0 | 27.00 | 13.55 | 1.99 |
| 5 | 200x51x1.15x0.95 | 1.0 | 1.2 | 21.75 | 7.67 | 2.84 |
| 6 | 250x51x1.15x1.15 | 1.0 | 1.0 | 28.50 | 10.23 | 2.79 |
| 7 | 250x51x1.15x0.95 | 1.0 | 1.2 | 23.25 | 5.79 | 4.02 |
| 8 | 150x51x1.25x1.25 | 1.0 | 1.0 | 31.73 | 25.64 | 1.24 |
| 9 | 200x51x1.25x1.25 | 1.0 | 1.0 | 35.45 | 19.42 | 1.83 |
| 10 | 250x51x1.25x1.25 | 1.0 | 1.0 | 38.08 | 15.08 | 2.53 |
| 11 | 150x51x0.95x0.95 | 1.5 | 1.0 | 14.25 | 8.30 | 1.72 |
| 12 | 150x51x1.15x0.95 | 1.5 | 1.2 | 15.00 | 8.30 | 1.81 |
| 13 | 200x51x0.95x0.95 | 1.5 | 1.0 | 16.25 | 5.85 | 2.78 |
| 14 | 200x51x1.15x0.95 | 1.5 | 1.2 | 18.80 | 5.85 | 3.21 |
| 15 | 250x51x1.15x0.95 | 1.5 | 1.2 | 19.38 | 4.41 | 4.39 |
| 16 | 150x51x1.25x1.25 | 1.5 | 1.0 | 26.95 | 20.98 | 1.28 |
| 17 | 200x51x1.25x1.25 | 1.5 | 1.0 | 29.50 | 15.07 | 1.96 |
| 18 | 250x51x1.25x1.25 | 1.5 | 1.0 | 31.98 | 11.60 | 2.76 |
| 19 | 150x51x1.15x0.70 | 1.5 | 1.6 | 13.75 | 3.94 | 3.49 |
| 20 | 200x51x1.15x0.70 | 1.5 | 1.6 | 15.50 | 2.78 | 5.58 |
| 21 | 150x51x1.15x1.50 | 1.0 | 0.7 | 41.25 | Combined | Combined |
| 22 | 150x51x1.15x1.90 | 1.0 | 0.6 | 35.00 | Combined | Combined |
| 23 | 150x51x1.15x1.15 | 1.5 | 1.0 | 18.25 | Combined | Combined |
| 24 | 250x51x1.15x1.15 | 1.5 | 1.0 | 24.00 | Combined | Combined |
| Mean | | | | | | 2.58 |
| COV | | | | | | 0.441 |

Note: Test Specimens 21 to 24 failed by combined bending and shear actions.

**Table 3: Comparison of Shear Capacities of Rivet Fastened RHFCBs with Proposed Equations**

| Test No. | RHFCB Section ($d \times b_f \times t_f \times t_w$) | $a/d_1$ | $t_f/t_w$ | Shear Capacity (kN) | | | Test/Eqs. 14 to 16 | Test/Eqs. 18 and 19 |
|---|---|---|---|---|---|---|---|---|
| | | | | Test | Eqs. (14) to (16) | Eqs. (18) and (19) | | |
| 1 | 150x51x0.95x0.95 | 1.0 | 1.0 | 17.00 | 15.53 | 14.66 | 1.09 | 1.16 |
| 2 | 150x51x1.15x1.15 | 1.0 | 1.0 | 23.75 | 21.64 | 20.48 | 1.10 | 1.16 |
| 3 | 200x51x0.95x0.95 | 1.0 | 1.0 | 20.08 | 17.22 | 17.37 | 1.17 | 1.16 |
| 4 | 200x51x1.15x1.15 | 1.0 | 1.0 | 27.00 | 24.81 | 24.35 | 1.09 | 1.11 |
| 5 | 200x51x1.15x0.95 | 1.0 | 1.2 | 21.75 | 17.22 | 17.37 | 1.26 | 1.25 |
| 6 | 250x51x1.15x1.15 | 1.0 | 1.0 | 28.50 | 27.45 | 27.85 | 1.04 | 1.02 |
| 7 | 250x51x1.15x0.95 | 1.0 | 1.2 | 23.25 | 19.75 | 19.83 | 1.18 | 1.17 |
| 8 | 150x51x1.25x1.25 | 1.0 | 1.0 | 31.73 | 28.61 | 27.04 | 1.11 | 1.17 |
| 9 | 200x51x1.25x1.25 | 1.0 | 1.0 | 35.45 | 33.85 | 32.86 | 1.05 | 1.08 |
| 10 | 250x51x1.25x1.25 | 1.0 | 1.0 | 38.08 | 36.62 | 37.08 | 1.04 | 1.03 |
| 11 | 150x51x0.95x0.95 | 1.5 | 1.0 | 14.25 | 14.83 | 14.06 | 0.96 | 1.01 |
| 12 | 150x51x1.15x0.95 | 1.5 | 1.2 | 15.00 | 14.83 | 14.06 | 1.01 | 1.07 |
| 13 | 200x51x0.95x0.95 | 1.5 | 1.0 | 16.25 | 16.40 | 16.63 | 0.99 | 0.98 |
| 14 | 200x51x1.15x0.95 | 1.5 | 1.2 | 18.80 | 16.40 | 16.63 | 1.15 | 1.13 |
| 15 | 250x51x1.15x0.95 | 1.5 | 1.2 | 19.38 | 19.13 | 18.96 | 1.01 | 1.02 |
| 16 | 150x51x1.25x1.25 | 1.5 | 1.0 | 26.95 | 28.02 | 26.48 | 0.96 | 1.02 |
| 17 | 200x51x1.25x1.25 | 1.5 | 1.0 | 29.50 | 31.62 | 31.22 | 0.93 | 0.95 |
| 18 | 250x51x1.25x1.25 | 1.5 | 1.0 | 31.98 | 34.85 | 35.39 | 0.92 | 0.90 |
| *19 | 150x51x1.15x0.70 | 1.5 | 1.6 | 13.75 | 9.88 | 9.97 | 1.39 | 1.38 |
| *20 | 200x51x1.15x0.70 | 1.5 | 1.6 | 15.50 | 11.81 | 11.74 | 1.31 | 1.32 |
| Mean | | | | | | | 1.06 | 1.08 |
| COV | | | | | | | 0.087 | 0.086 |

Note: * Tests 19 and 20 were not considered in the design equations as the flange to web thickness ($t_f/t_w$) ratio exceeds the limit of proposed design equations ($t_f/t_w < 1.2$).

**Table 4: Shear Yielding and Buckling Capacities of Rivet Fastened RHFCBs**

| Test No. | RHFCB Section ($d x b_f x t_f x t_w$) | Test $V_v$ (kN) | $V_y$ (kN) | $V_{cr}$ (kN) | $V_V/V_y$ | $\lambda$ |
|---|---|---|---|---|---|---|
| 1 | 150x51x0.95x0.95 | 17.00 | 18.53 | 13.92 | 0.92 | 1.15 |
| 2 | 150x51x1.15x1.15 | 23.75 | 23.94 | 24.59 | 0.99 | 0.99 |
| 3 | 200x51x0.95x0.95 | 20.08 | 26.28 | 9.81 | 0.76 | 1.64 |
| 4 | 200x51x1.15x1.15 | 27.00 | 33.96 | 17.33 | 0.79 | 1.40 |
| 5 | 200x51x1.15x0.95 | 21.75 | 26.28 | 9.81 | 0.83 | 1.64 |
| 6 | 250x51x1.15x1.15 | 28.50 | 45.01 | 13.07 | 0.63 | 1.86 |
| 7 | 250x51x1.15x0.95 | 23.25 | 34.83 | 7.40 | 0.67 | 2.17 |
| 8 | 150x51x1.25x1.25 | 31.73 | 30.36 | 36.70 | 1.04 | 0.91 |
| 9 | 200x51x1.25x1.25 | 35.45 | 44.88 | 24.83 | 0.79 | 1.34 |
| 10 | 250x51x1.25x1.25 | 38.08 | 57.76 | 19.29 | 0.66 | 1.73 |
| 11 | 150x51x0.95x0.95 | 14.25 | 18.53 | 11.80 | 0.77 | 1.25 |
| 12 | 150x51x1.15x0.95 | 15.00 | 18.53 | 11.80 | 0.81 | 1.25 |
| 13 | 200x51x0.95x0.95 | 16.25 | 26.28 | 8.32 | 0.62 | 1.78 |
| 14 | 200x51x1.15x0.95 | 18.80 | 26.28 | 8.32 | 0.72 | 1.78 |
| 15 | 250x51x1.15x0.95 | 19.38 | 34.83 | 6.27 | 0.56 | 2.36 |
| 16 | 150x51x1.25x1.25 | 26.95 | 31.57 | 29.91 | 0.85 | 1.03 |
| 17 | 200x51x1.25x1.25 | 29.50 | 44.09 | 21.42 | 0.67 | 1.43 |
| 18 | 250x51x1.25x1.25 | 31.98 | 57.39 | 16.46 | 0.56 | 1.87 |
| *19 | 150x51x1.15x0.70 | 13.75 | 15.10 | 5.60 | 0.91 | 1.64 |
| *20 | 200x51x1.15x0.70 | 15.50 | 21.43 | 3.95 | 0.72 | 2.33 |

Note: * Tests 19 and 20 were not considered in the design equations as the flange to web thickness ($t_f/t_w$) ratio exceeds the limit of proposed design equations ($t_f/t_w < 1.2$).